ISSN 1840-4855
e-ISSN 2233-0046

Original scientific article
http://dx.doi.org/10.70102/afts.2026.1836.434

EFFICIENTNET-B0-BASED FRAMEWORK FOR AUTOMATED MULBERRY ROOT KNOT DISEASE CLASSIFICATION BASED ON LEAF SYMPTOMS USING GRAD-CAM VISUALIZATION

N. Priyanka[1*], Dr.K.G. Mohan[2]

[1]Research Scholar & Assistant Professor, GITAM School of Computer Science & Engineering, GITAM (Deemed to be University), Doddaballapur, Bengaluru, Karnataka, India. e-mail: pnarayan@gitam.edu, orcid: https://orcid.org/0000-0003-2851-6714*
[2]Professor, GITAM School of Computer Science & Engineering,
GITAM (Deemed to be University), Doddaballapur, Bengaluru, Karnataka, India.
e-mail: mkabadi@gitam.edu, orcid: https://orcid.org/0000-0002-9975-1773

Received: May 16, 2026; Revised: June 27, 2026; Accepted: August 07, 2026; Published: September 29, 2026

SUMMARY

The study is based on the idea of an innovative method of automated classification of mulberry root Knot diseases on the basis of the leaf symptoms through the EfficientMulberryNet-B0-GC model, which is a combination of EfficientNet-B0 and Grad-Cam visualization. The model aims to complement the lack of efficient and transparent disease detection in agricultural practices and offer a strong solution for real-time classification of mulberry root knot disease according to leaf symptoms. The method proposed uses a dataset of mulberry leaves that consists of high-resolution images of two classes, i.e., Healthy, Root knot disease. The EfficientMulberryNet-B0-GC model, which is pre-trained on ImageNet, is then fine-tuned to classify diseases with data augmentation techniques used to enhance the generalization of the model. It makes the model's decision-making process transparent and more credible by using the technique of Grad-CAM to visualize and interpret the model's decision-making process. The results indicate that the proposed model outperforms existing models as it attains 94% accuracy, 95% precision, 95% recall, 95% F1 score, and 99% AUC. The data set is of 2500 images, diversified to be strong and extensive. The framework provides a scalable, practical approach to disease monitoring to provide improved disease accuracy, interpretability, and reliability. The study helps to develop AI-based tools in the agricultural sector, especially the detection and management of diseases in the mulberry.

Key words: *mulberry root knot disease, efficientmulberrynet-B0-GC, disease classification, grad-cam visualization, deep learning, plant health monitoring, agricultural AI.*

INTRODUCTION

Mulberry (Morus spp.), is a fast-growing, deciduous, perennial tree crop widely grown in tropical, subtropical, and temperate regions of Asia, Africa, and South America. The crop is significant from a socio-economic point of view, as it is the sole natural food source for Bombyx mori L., an insect of the sericulture industry, which is the reason why the productivity and quality of mulberry leaves are directly related to the yield of cocoons and quality of silk in the sericulture industry. Apart from the production

of silk, leaves and fruits of mulberry are utilized in traditional medicine, animal feed, and functional food products; the crop's health is thus closely connected with the livelihood of millions of farmers in the countries where mulberry is cultivated, including India and China. Mulberry is susceptible to many root diseases, including those caused by soil-borne fungi, bacteria, and plant-parasitic nematodes, like other perennial crops. Root diseases are especially serious because strike below-ground parts of plants that take in water and nutrients. When above-ground symptoms like wilting, yellowing, or stunted growth first become evident, a root system may be so severely damaged that the disease has already become difficult to manage and control in a timely manner.

Root knot disease, which is caused by root-knot nematodes (RKNs) of the genus Meloidogyne, mainly Meloidogyne incognita, is considered one of the most economical root diseases of mulberry among the many types of root diseases. Root-knot nematodes penetrate into the root tissue and cause the development of galls that compress the vascular system and lead to the inability of other parts of the plant to carry water and nutrients. This ultimately results in a diminished production of silk cocoons with a smaller size and less biomass of leaves fed by the silkworms, causing a direct economic loss for sericulture farmers. Root knot disease is prioritized in this study over other root ailments because it is widespread across sericulture-growing regions, difficult to diagnose early since the nematodes remain hidden underground, and severe enough in its downstream impact to justify a dedicated, non-destructive, image-based early-warning system built around the indirect leaf-level cues that it produces.

Conventionally, root knot disease has been diagnosed by uprooting plants and visually inspecting the root system for characteristic galls, followed by laboratory confirmation through nematode morphological identification, perineal pattern microscopy, or molecular techniques such as PCR and rDNA-ITS sequencing. While these traditional approaches remain a reliable basis for species-level confirmation, destructive to the plant, time-consuming, dependent on the availability of trained nematologists, and unsuitable for continuous, large-scale, or real-time field monitoring, particularly in the resource-constrained sericulture settings where early detection is most needed. These limitations have motivated a shift toward machine learning and deep learning-based approaches that can classify plant diseases directly from images, offering a faster and non-destructive alternative to conventional diagnosis.

To suggest a hybrid CNN-ViT model to detect mulberry leaf Root knot disease and incorporate explainable AI (XAI) to enhance the transparency and interpretability of the model. This method has the advantage of improving the level of detection as well as the credibility of the system, thereby providing a valid solution to monitoring plant diseases [1]. This paper presents HVAF-XAI-Net, a multimodal explainable AI model that provides accurate detection of mulberry leaf Root knot disease. This framework enhances the diagnostic's performance by integrating several AI methods, offering a powerful solution for monitoring plant health with attention to interpretability [2]. To design a CNN model that is lightweight and can be used to classify jute leaf Root knot disease in real time. Their model includes a supervised and semi-supervised self-training model, which improves the speed and precision of disease classification and is applicable in real-time in agricultural practices [3]. The survey aims to perform an in-depth survey on explainable AI (XAI) in plant health monitoring. Their work shows the issues and possibilities of applying XAI methods, and the importance of transparency in AI systems to increase user trust and decision-making in agricultural contexts [26][4]. In this, a ResNet152 is employed with the help of Grad-CAM to improve the diagnosis of corn leaf disease. Which is enhance the precision of disease diagnosis and the understandability of the model, providing insights into the workings of the AI system [5][6]. To present DELG Net, a two-stream cross-attention model to identify nutrient deficiencies in mulberry leaves automatically. The framework has shown better results in terms of finding nutrient deficiencies, indicating the opportunities of the advanced AI models to apply to agriculture [27]. suggested the Mamba-YOLO-ML framework, a state-space model-based method of detecting the disease in mulberry leaf. The technique combines the strengths of state-space modeling with the YOLO framework, boosting the precision and reliability of the disease recognition of mulberry leaves, and is applicable to real-world farming scenarios [3]. The model also has an enhanced performance in that it addresses the differences in environmental conditions effectively [7].

Agricultural disease detection has made some major breakthroughs with the use of AI models. For example, came up with explainable hybrid knowledge-based and data-driven AI structures, which help to improve the diagnosis of faults within cyber-physical systems. This can be employed in plant disease detection in agriculture [10]. Also, to employ the use of data augmentation using DCGAN on tomato leaf disease identification, thus making the system much stronger [11]. Further, to introduce a model for identifying tomato leaves disease named LBFNet. This is a tomato leaf disease identification model that uses a three-channel attention mechanism and quantitative pruning [12]. Moreover, to combine the deep learning approach and GIS for car maintenance predictions. This can also play an important role in automobile maintenance prediction in agriculture [13]. Furthermore, to apply a deep neural network model to automatically detect the disease present on the fruits and leaves of a citrus tree. This can help to show the versatility of deep learning in agriculture [14]. Finally, in this work, to enhance tomato leaf disease identification with Inception V3 and two kinds of attention mechanisms [15].

To suggest a combination of CNNs using fusion and Grad-CAM to identify plant diseases reliably and transparently. To take the best of several models and increase the reliability and interpretability of AI systems deployed in monitoring plant health [8]. The higher quality monitoring of fruits through the combination of non-destructive technologies and artificial intelligence. Their research seeks to improve the quality assessment of fruits, and so it is a significant contribution to the sustainable and accurate production of fruits [9]. YOLO-SDA, a new version of YOLOv12, is an architecture that is presented in this paper to classify peanut foliar diseases. This model is better than the old technique, which gives better accuracy of detection and is a good technique to effectively control the disease in crops [28]. Here, various researchers provide important contributions through various fields of AI with XAI to detect plant diseases. To integrate the various models with AI deep learning models related to the various techniques, such as Grad-CAM. It's for enhancing the various metrics through productive types of agricultural practices [29][30].

Although various achievements have been made, the current AI-based plant disease detection systems still have some drawbacks in the context of mulberry root knot disease. The first is most previous deep learning research focused on superficial (visually observable) leaf disease rather than root diseases that must be deduced from other indicators on the leaves, which has been previously missing with systemic root distress detection. Second, many high-performing models are large and/or compute intensive, making them impractical to deploy on the types of low-power, edge devices at the disposal of many smallholder farmers. Third, many models are opaque black boxes and do not provide information about how they make predictions, which reduces the confidence of agricultural stakeholders and also stifles the use of models in practice-driven agricultural extension services. Finally, there are limited datasets of mulberry root knot disease that are freely available and well-annotated, limiting the scope and transferability of models that are trained for this particular purpose.

To resolve these issues, this paper introduces the EfficientMulberryNet-B0-GC framework, a lightweight and interpretable deep-learning framework comprising a transfer-learned EfficientNet-B0 backbone and a Grad-CAM visualization for automatic mulberry root knot disease classification based on mulberry leaf images. EfficientNet-B0 is chosen as the backbone due to the compound scaling strategy and the mobile inverted-bottleneck design, which provides a steep enough parameter growth curve to achieve a good classification accuracy-to-computation ratio suitable for application on resource-poor devices in the field. The backbone is pre-trained on ImageNet, fine-tuned on an extended set of images of mulberry leaves from healthy and root-knot-infected plants, and Grad-CAM is overlaid on these to show the regions of the leaf where the IT most influenced each prediction, creating a clear and visually interpretable ground for farmers and agronomists to trust and act on the model's output.

Objective of the Study

- To develop a lightweight, transfer-learning-based EfficientNet-B0 model capable of accurately classifying mulberry leaves as healthy or affected by root knot disease using only leaf-level images.
- To integrate Grad-CAM visualization into the classification pipeline so that the leaf regions driving each prediction are transparent and interpretable to end users.

- To evaluate the proposed EfficientMulberryNet-B0-GC framework against existing state-of-the-art models using standard performance metrics such as accuracy, precision, recall, F1-score, and AUC.
- To provide a scalable, real-time, and field-deployable solution for the early, non-destructive detection of mulberry root knot disease in support of sustainable sericulture practices.

Key Contribution

- **State-Space Model Integration:** The article presents a new approach to integrating state-space modelling and the YOLO structure, enhancing the quality and reliability of mulberry Root Knot disease detection based on leaf symptoms.
- **Enhanced Detection Performance:** The framework improves the detection performance of the model to identify mulberry leaf root knot diseases in different environmental conditions using the state-space approach.
- **Real-World Applicability:** The Mamba-YOLO-ML model is created to be used in practical, real-time applications in agriculture, and is a stable model that can be used in real-world environments to monitor the health of plants.
- **Model Robustness:** The model is very robust to environmental noise and variation; it is guaranteed to perform well even under complex and dynamic agricultural conditions.

This research report covers by the following sections, Section I explained about introduction about the topic, Section II explained about the literature review included with research gap, Section III explained about proposed Methodology followed by the overall architecture of proposed methodology, Working Principle for Efficient B0 based Framework, Automated Mulberry Root Disease classification based on leaf symptoms using GRAD-CAM visualizations, Data flow diagram about proposed methodology and proposed Algorithms. Section IV explained about results, and the discussion section consists of dataset description, Software and Hardware details, Parameter initialization, Metric Evaluation of various models, Performance comparison for the proposed model with various models, performance evaluation of the proposed Model, ROC Curve Evaluation, Training Accuracy, Training loss, Ablation study analysis. Section V presented the research's conclusion.

LITERATURE REVIEW

A range of recent studies has explored automated, image-based detection of root-knot nematode (RKN) infestation across crops, spanning object-detection architectures, convolutional classifiers, and non-imaging sensing techniques. The surveyed studies collectively demonstrate a strong shift toward automated, AI-driven detection approaches, encompassing deep learning architectures such as YOLOv5, YOLOv7, YOLOv8, CNN-based models including AlexNet, VGG16, EfficientNet V2-S, ResNet101, and Swin Transformer, as well as hyperspectral remote sensing and traditional digital image analysis methods. Species-level identification of root-knot nematodes is normally based on subtle differences in the perineal pattern, the pattern of striae surrounding the vulva and anus of the adult female, and correct species discrimination matters because different Meloidogyne species vary in host range and pathogenicity; Khan et al. [16] automated this perineal-pattern-based species identification for six RKN species using a YOLOv8 model, while Das et al. [17] built a CNN framework on AlexNet and VGG16 to distinguish M. graminicola, M. incognita, and M. javanica from the same type of microscopic imagery, reporting approximately 95% accuracy. Root knot severity in field crops is conventionally graded from the visible extent of root galling caused by nematode feeding sites, and Zhao et al. [18] proposed Root-YOLOv7 to grade root-knot disease severity directly from gall imagery in cucumber roots, attaining an AP@0.5 of 87.40%. Rangarajan et al. [19] extended nematode identification beyond a single genus, applying EfficientNet V2-S and Swin Transformer V2-B to distinguish seven plant-parasitic nematode genera, including root-knot nematodes, from turfgrass soil samples. Because nematodes are too small to identify in the field with the naked eye, Singh et al. [20] developed a lightweight, mobile-deployable CNN application that lets farmers identify nematodes on-site from microscopic images without specialist assistance, reporting over 98% accuracy. Counting the egg and juvenile life stages of Meloidogyne spp. in root and soil samples is a routine but labour-intensive step used to estimate nematode population density and guide management decisions; Saikai et al. [21] addressed this with the open-source SEGNEMA pipeline built on YOLOv8x, while Agarwal et al. [22]

compared CNN, contour-based, and hybrid image-analysis pipelines for the same egg-counting task relevant to screening plant germplasm for nematode resistance, with the hybrid approach reaching R^2 = 0.992 for M. incognita. In tomato, root-knot disease is assessed from the number of galls, egg masses, and juveniles present on the root system: Pun et al. [23] compared YOLOv2 through YOLOv7 for this gall-and-juvenile detection task, packaged the resulting model into a web-based decision support tool, NemDST, to help growers interpret nematode counts and time interventions [24], and earlier introduced digital image analysis methods, including a Skeleton Graph technique, to quantify root-knot galling directly on tomato roots [28]. Reflecting the destructive and difficult-to-diagnose nature of plant-parasitic nematode disease across crops, Pun et al. [25] reviewed 44 studies spanning morphological, PCR/metabarcoding, hyperspectral, and deep-learning-based nematode identification and management technologies. Root-knot infection affects root and canopy physiology before any symptoms appear on the foliage, so Waghmare [26] employed a handheld spectroradiometer to monitor the reflectance of the canopy over a range of 350–1600 nm to identify an early non-destructive indicator of M. incognita in mungbean, while Žibrat et al. [27] employed hyperspectral imaging combined with dimensionality-reduction techniques and an SVM classifier to detect an infestation of potato tubers with the quarantine pathogen M. luci without cutting into them. All these studies suggest that machine learning and computer vision have the potential to considerably replace the manual nematode identification, which is a labor-intensive task, providing more accurate, efficient, and scalable root-knot disease management in agricultural systems.

The EfficientMulberryNet-B0-GC framework proposed fills a missing gap in the literature, which mostly deals with superficial leaf pathogens. Lightweight, interpretable frameworks to identify systemic root distress using indirect foliar cues do not exist, particularly on edge devices limited by resources. The study combines Grad-CAM visualization to obtain transparency, a varied dataset of mulberry leaves data augmented to achieve better robustness, and transfer learning with EfficientNet-B0 to achieve better classification outcomes. The framework provides a realistic, real-time solution to plant health monitoring in sericulture by addressing the issue of mulberry root knot diseases, enhancing the accuracy of the diagnostic and interpretability of the model.

PROPOSED METHODOLOGY

Overall Architecture of Proposed Methodology

The proposed model architecture depicted through the diagram figure 1 below is one that seeks to automate classification for mulberry root Knot diseases through the use of EfficientNet-B0 along with Grad-CAM visualization. First, collect mulberry leaf image datasets representing the two classes, namely, healthy leaves (Class 0), Root knot disease (Class 1). Image datasets are pre-processed through scaling of dimensions to 224 x 224 pixels, rescaling of pixel values by dividing by 255, and, when required, denoising the dataset. Datasets are further partitioned into training sets of 80%, validation sets of 10%, and test datasets of 10%.

The EfficientNet-B0 structure, which has been pre-trained on ImageNet through the application of the transfer learning idea, serves as the model's central pillar. Both dropout (0.2), which serves to avoid overfitting, and global average pooling, which reduces the size of the feature map, are crucial components of this neural network. Both of these components are included in this neural network. One thing to keep in mind is that this structure uses the fully linked layer and the softmax function to categorize photos. To make the dataset bigger, to use data augmentation on the training data. This involves techniques like flipping and rotating images. Then, the Grad-CAM method is used to show which parts of the leaf images the model focuses on when making predictions. This helps us understand how the model makes its decisions.

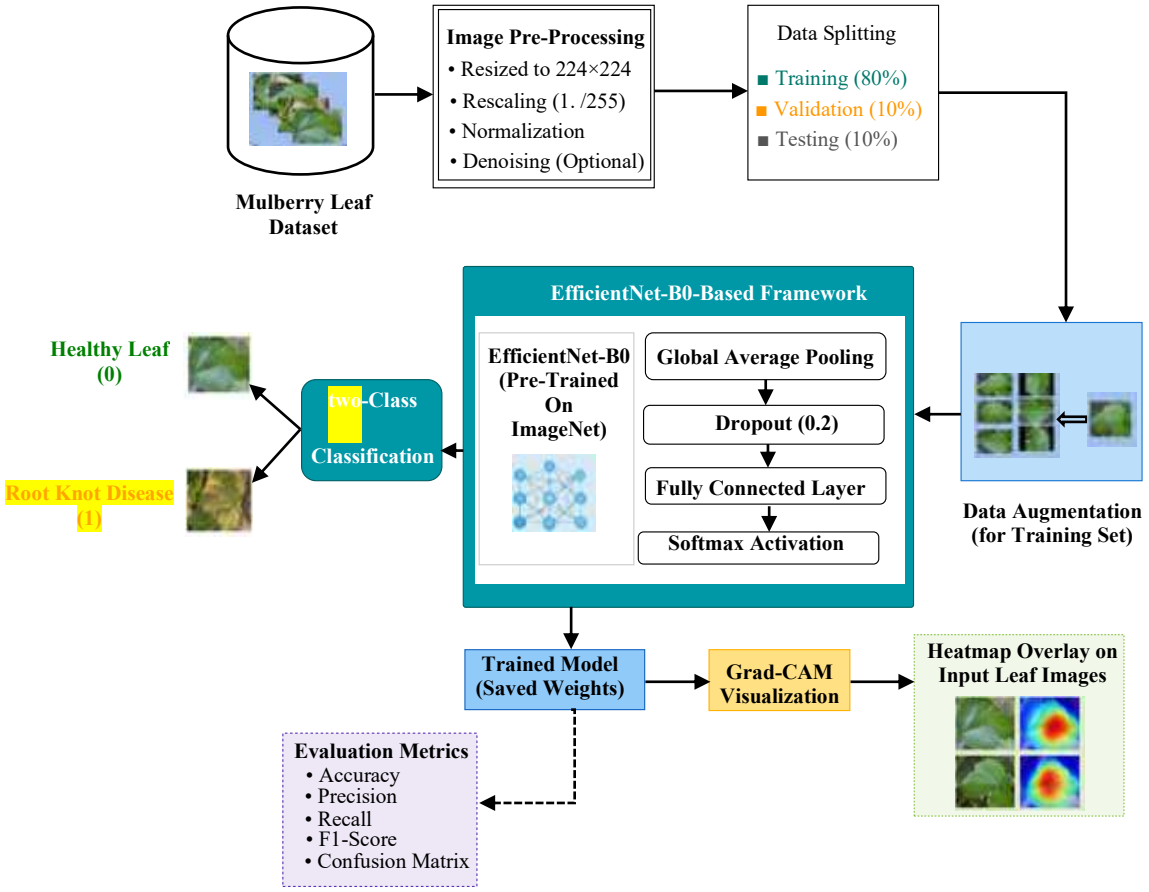

Figure 1. Overall architecture diagram of the proposed methodology

Working Principle for Efficientnet-B0-Based Framework

EfficientNet-B0 serves as the base model in the EfficientNet family. EfficientNet-B0 has proved to be highly successful in the task of image classification. The framework of EfficientNet-B0 incorporates a method of scaling that allows for uniform scaling of dimensions as well as resolution in figure 2.

Mobile Inverted Bottleneck Convolution (MBConv) components serve as the foundation for the EfficientNet-B0 design, which also incorporates squeeze-and-excitation (SE) blocks. While simultaneously reducing the total number of parameters, this design provides an efficient way to achieve maximum precision. It includes depth-separable convolution to decrease computational complexity by a factor of K^2. In which K represents the kernel size. Additionally, the architecture has inverted residual blocks, which bring the total number of trainable parameters down to a lower level. EfficientNet-B0 scales depth, width, and resolution to ensure optimal model scaling. Compound scaling involves the utilization of a compound coefficient denoted by þ, which is stated by equation (1).

$$d = \propto \psi, \omega = \beta\psi, \gamma = \gamma\psi \qquad (1)$$

From the above equation (1) describes as $\propto \geq 1, \beta \geq 1 \; and \; \gamma \geq 1$ These are all as scaling factors. To determine these values based on grid search and $\emptyset$ depends upon the model scaling.

The Swiss function is defined as equation (2) as follows,

$$fswiss(x) = \frac{x}{1 + e^{-\beta(x)}} \qquad (2)$$

The last layer of the EfficientNet-B0 design, represented by equation (2), is likewise accountable for forecasting the final classification result using the features retrieved from the layers that came before it.

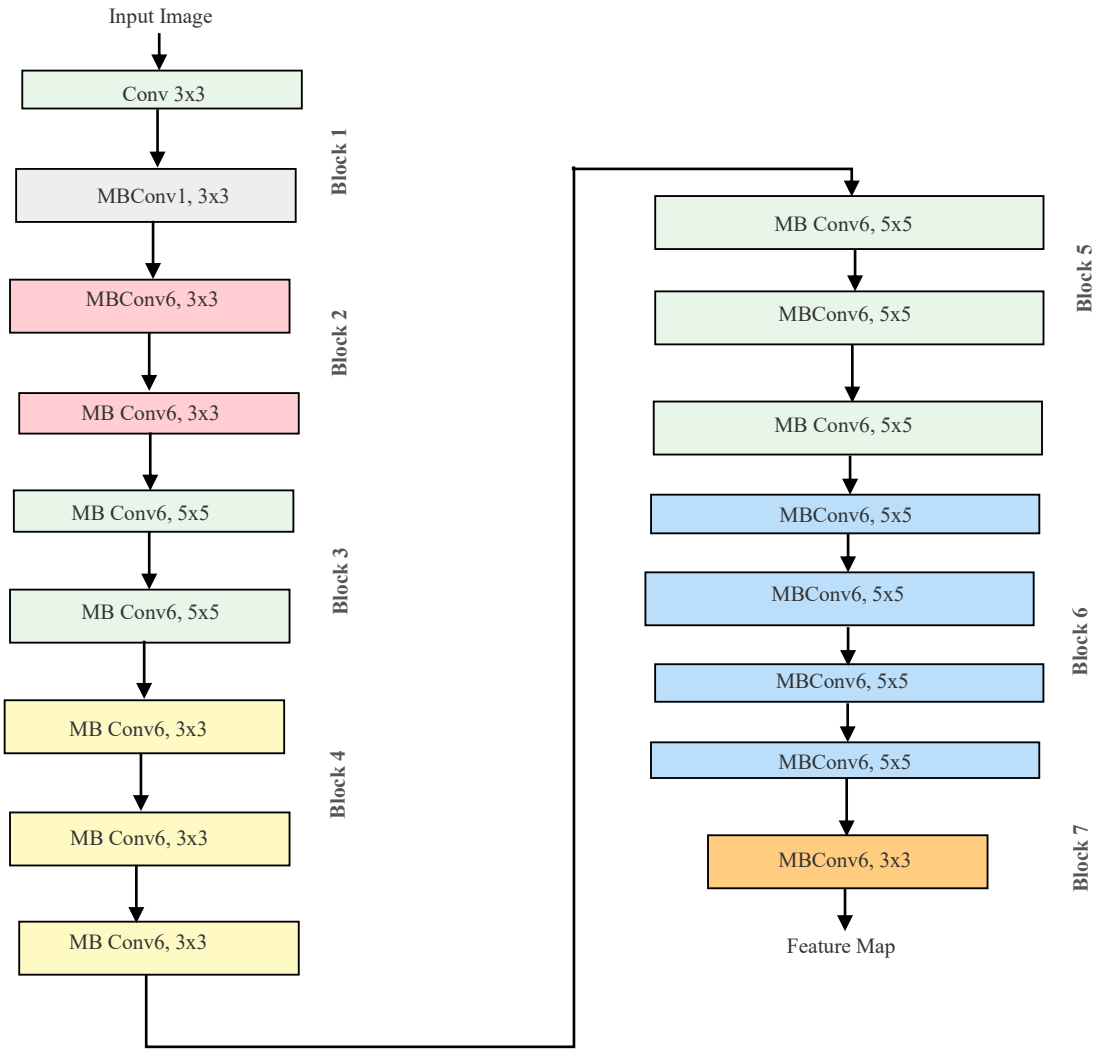

Figure 2. Working principle for efficientnet-B0-Based framework

Fine-Tuned Efficientnet-B0 Model

In this part, the EfficientNet-B0 model that has been fine-tuned is presented. Importing the Keras library was done in order to prepare the EfficientNet-B0 for training. It was necessary to train the network using a total of 241 layers. Extraction of features was accomplished by utilizing the architecture's many layers. Improved performance over the baseline EfficientNet-B0 model was achieved by modifying the final three layers of the model to accommodate transfer learning. To make use of a convolutional window in two dimensions.

Automated Mulberry Root Knot Disease Classification Based on Leaf Symptoms Using Grad-Cam Visualization

Figure 3 shows the general outline of the improved Grad-CAM that uses Dropkey: To eliminate superfluous signals and conceal a specific percentage of attention weights, the Dropkey algorithm adds a Bernoulli noise layer to the attention score matrix. This reduces the risk of relying too much on a single local piece of data for the neural network model. To get the weight coefficients, Dropkey does the softmax operation along the attention score matrix's last dimension. The weights and averages of the value vectors are calculated using these coefficients. Finally, the query is encoded and retrieved as a weighted average. The text within the dashed box contains information about how Drop key's Q, K, and V parameters work.

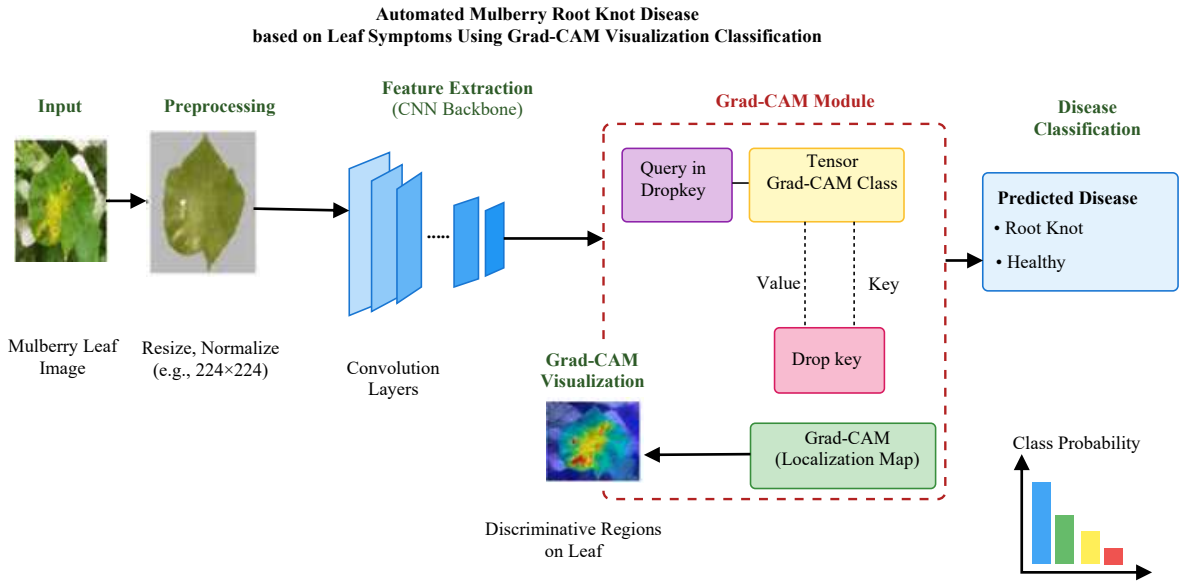

Figure 3. Automated mulberry root knot disease classification based on leaf symptoms using Grad-CAM visualization

To lessen the dependence on specific neurons in Grad-CAM computation, the Dropkey attention approach incorporates random binary masks. To be more specific, during the process of computing weights for attention, a shape-matching binary random mask tensor is multiplied element-wise with the attention. In addition, the attention weights on the masked positions are multiplied by a small undesirable value, and the result is set to negative infinity. This reduces their impact on the final visual interpretability results by making sure the attention weights at the disguised places are effectively zero following the softmax process. To further enhance the generalizability of the results of visual interpretation, the Dropkey approach also removes a fraction of the neurons at random. The utilization of this approach allows Grad-CAM to become more effective in handling various input samples, which in turn improves its performance in terms of generalization on the overall sample. A more thorough reflection of the representation's focus on the mark feature regions is thus achieved in the produced heatmaps. The Dropkey technique introduces accidental masks and neuron Dropout, which change the distribution of attention weights, in contrast to Grad-CAM, which is improved with Dropout. Improved stability and interpretability of heat maps are the results of increasing the attention weights' unpredictability. In general, the upgraded Dropkey Grad-CAM is more stable and is able to generalize better. This helps to better grasp how the model makes decisions and what attributes of the input picture are emphasized in the model. As a consequence, the explanations of model predictions are made more accurate, reliable, and interpretable.

Grad-CAM can be comprehensively explained through mathematical derivation. By differentiating the output y^c of category c with respect to the feature map of the convolution layer, the gradient information for each category in the image can be obtained as $\partial y^c / \partial A^k$ where A^k represents the Grad-CAM class activation map. To apply backpropagation, use the gradient information from equation (4). Based on the prediction result, the vector should be represented by

Y, y^c and the score of the target class c, it can be obtained through the output of the connected layer in the softmax network, depending upon the task.

$$\alpha_k^c = \frac{1}{Z}\sum_i \sum_j \frac{\partial y^c}{\partial A_{ij}^k} \qquad (3)$$

Equation (3) describes the $\propto_k^c$ It refers to the linearization coefficient in the later part of the neural network model. It also represents the weight information of the feature map k for a specific class c, where Z is the number of channels.

$$L^C = ReLU\left(\sum_K \propto_k^c A^K\right) \qquad (4)$$

From the above equation (4) describes and detects the various combinations among the forward conditions achieved through ReLu in activation functions. This heatmap should contain the size of the convolution through the feature map obtained in the above equation (4).

GRAD-CAM uses the input data to calculate the output layer's feature map and the gradients for each category. The gradients of all channels are averaged and weighted, and the positive weights from each category are summed. These computations are then used to create a heat map. The heatmap shows the weight for each pixel of the selected category. To create the heatmap, first add together all of the positive weights from all of the channels.

Dataflow Diagram for Proposed Methodology

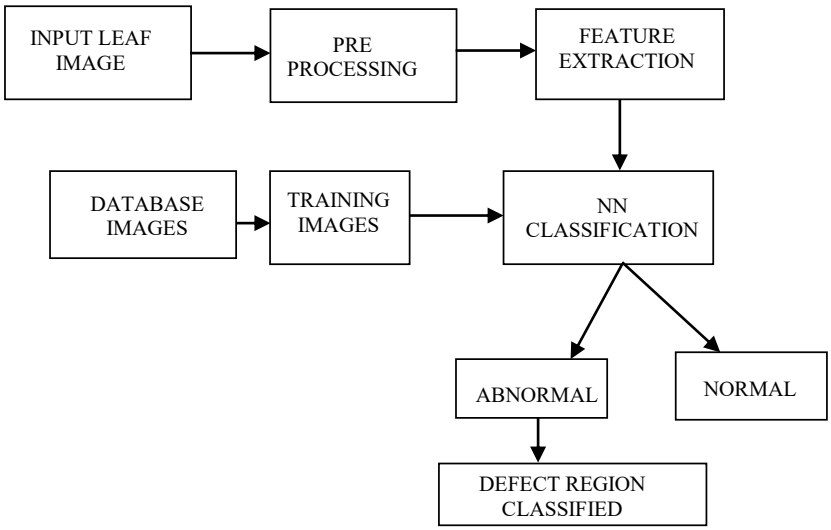

Figure 4. Data flow diagram of proposed methodology

The flowchart figure 4 represents a framework for classifying leaf Root Knot diseases based on image analysis. It begins with the input of a leaf image, followed by preprocessing steps. The preprocessing stage is crucial for preparing the image for the next step, which involves feature extraction. Once features are extracted, the system uses a neural network (NN) classification model to categorize the leaf as either "normal" or "abnormal." If the leaf is classified as abnormal, the system further analyzes the defect region and classifies it. Database images are used for training the system, ensuring that the model learns to distinguish between normal and abnormal leaf conditions based on the features extracted from the images.

Proposed Algorithm

Algorithm-1

Find the best threshold λd for disease detection to achieve the highest select accuracy and coverage using EfficientNet-B0 and Grad-CAM

1: $function\ THRESHOLD_ESTIMATION(ytrue, ypred, P, \beta, model, image_data)$

2: $\chi incorrect \leftarrow ytrue \neq ypred$

3: $pmax \leftarrow max(P).$

4: $\lambda possible \leftarrow unique(pmax[\chi incorrect]).$

5: $\lambda best \leftarrow 0$

6: $SAbest \leftarrow 0$

7: $SELbest \leftarrow 0$

8: $for\ \lambda \in \lambda possible\ do$

9: $Select \leftarrow Pmax$

10: $Reject \leftarrow Pmax$

11: $Rejindex \leftarrow (ytrue \neq ypred)[Rejindex]$

12: $n \leftarrow count(Rejindex)$

13: $k \leftarrow count(Rejindex, k, n, p)$

14: $prob \leftarrow binom.cdf(k, n, p)$

15: $if\ prob \leq 1 - \beta\ then$

16: $SA \leftarrow accuracy(ytrue[Select], ypred[Select])\ .$

17: $SEL \leftarrow count(Select)$

18: $end\ if$

19: $if\ (SA > SAbest)\ or\ (SA = SAbest\ and\ SEL > SELbest)\ then$

20: $\lambda best \leftarrow \lambda$

21: $SAbest \leftarrow SA$

22: $SELbest \leftarrow SEL$

23: $end\ if$

24: $end\ for$

25: $for\ image\ in\ image_data\ do$

26: $prob_map \leftarrow model.predict(image)$

27: $GradCAM \leftarrow generate_gradcam_map(model, image)\ .$

28: $overlay_gradcam(image, GradCAM)$

29: $end\ for$

30: $return\ \lambda best$

31: $end\ function$

The algorithm 1 focuses on determining the best value for threshold (λd) that will optimize accuracy (SA) and coverage (SEL) for disease detection using EfficientNet-B0 and Grad-CAM. This algorithm first determines which predictions are wrong (line 2) and identifies possible thresholds based on maximum predicted probabilities (lines 3-4). It then calculates the selected predictions' accuracy and determines the number of selected predictions taking into account statistical significance (lines 14-17). The algorithm determines the optimal threshold by maximizing accuracy and, in cases where there is a tie between thresholds, chooses the one with more coverage (lines 19-23). With the optimal threshold having been found, it uses Grad-CAM to identify Class Activation Maps for all the images in the dataset (lines 25-29). The algorithm finally returns the threshold that has been identified (line 30).

Algorithm-2

Generate Grad-CAM Heatmap for Visualization

1: $function\ generate_gradcam_map(model, image)$

2: $conv_layer \leftarrow get_last_convolutional_layer(model)$.

3: $with\ tf.GradientTape()\ as\ tape$:

4: $tape.watch(image)$

5: $prediction \leftarrow model(image)$

6: $class_output \leftarrow prediction\ [0, class\ index]$.

7: $grads \leftarrow tape.gradient(class_output, conv_layer.output)$.

8: $pooled\ grads \leftarrow tf.reduce_mean(grads, axis = (0,1,2))$.

9: $heatmap \leftarrow tf.reduce_mean(conv_layer.output * pooled_grads, axis = -1)$.

10: $heatmap \leftarrow tf.maximum(heatmap, 0)$

11: $heatmap \leftarrow heatmap\ /\ tf.reduce_max(heatmap)$

12: $return\ heatmap$

13: $end\ function$

Algorithm 2 explained about generate_gradcam_map function creates a Grad-CAM heatmap for visualizing the areas of an image that contribute the most to the model's prediction. It first identifies the last convolutional layer in the model (line 2). Then, using TensorFlow's GradientTape, it tracks the operations on the image (line 4), computes the model's prediction (line 5), and extracts the output corresponding to the class of interest (line 6). The gradient of the class output with respect to the convolutional layer's output is calculated (line 7), and the gradients are averaged across the spatial dimensions (line 8). A heatmap is then generated by multiplying the averaged gradients with the convolutional layer's output (line 9), followed by normalization to keep the values between 0 and 1 (lines 10-11). The function returns the normalized heatmap (line 12), which highlights the areas of the duplicate that are most influential in the model's prediction.

Algorithm-3

Overlay Grad-CAM on Image

1: $function\ overlay_gradcam(image, GradCAM)$

2: $image_with_heatmap \leftarrow image + GradCAM$

3: $display(image_with_heatmap)$

4: $end\ function$

The Algorithm 3 mentioned the function overlay_gradcam displays the Grad-CAM heat map using an overlaying technique in which the heat map is overlaid onto the original image. In this operation, the heat map indicating the most important regions for the model's prediction is overlaid on the original image (line 2). This results in the formation of a single image containing both the original image and the areas that have the highest impact on the decision-making process. The final image is displayed as output (line 3).

RESULTS AND DISCUSSION

Dataset Description

The mulberry root Knot disease database contains 2500 high-resolution images of leaves from mulberry trees that display different symptoms of root diseases, such as Healthy, Fungal Root Rot, Bacterial Wilt, and Root-Knot Nematode. Each image has a uniform resolution of 160x160 pixels. In order to ensure an increase in the diversity of the database and improve the quality of the classification model, the process of artificial oversampling of data and geometric/colored transformations like rotating, zooming, and jittering is performed. As a result, the database becomes more versatile by simulating varied light conditions in the field. This helps to enrich the database and make it more robust [24].

Software and Hardware Details

Table 1. Software and hardware details

Configuration Parameter	Details
Software	TensorFlow, Keras, Python 3.x
Libraries/Tools	EfficientNet-B0, Grad-CAM, OpenCV
Operating System	Ubuntu 20.04 LTS
Programming Language	Python 3.x
Development Environment	Jupyter Notebook, PyCharm
Hardware	Intel i7 (8 cores, 3.0 GHz+)
Framework	Keras for deep learning model, OpenCV for image processing
Storage	100 GB SSD

Table 1 describes the software and hardware setup for mulberry root knot disease classification is robust and appropriate for carrying out deep learning operations. The software includes TensorFlow and Keras for developing the model, where Python 3.x will be used as the programming language. In addition, EfficientNet-B0 and Grad-CAM libraries will be used to develop the deep learning model and visualize the results, respectively. Meanwhile, OpenCV will be used to process images before feeding them to the deep learning algorithm. The operating system running the whole process is Ubuntu 20.04 LTS, which is ideal for machine learning tasks. Moreover, the software development tools that will be used include Jupyter Notebook and PyCharm. Regarding hardware, the machine contains an Intel i7 processor with 8 cores, 16GB RAM, and a NVIDIA GTX/RTX GPU with 8GB VRAM. There is also an SSD of 100 GB in size. Such specifications make the configuration capable of supporting the training of a deep learning model.

Parameter Initialization

Table 2 shows that the goal of initializing parameters in the mulberry root disease classification model is to improve how well it works with new data. All images are made the same size, 224x224, to keep everything consistent. The data is divided into three parts: training, validation, and testing. The training

and validation each get 80% of the data, and the testing gets 10%. During training, a value of 0.2 is used for dropout to stop the model from learning too much from the training data, which helps it perform better.

Table 2. Parameter initialization

Parameter	Value
Image Resolution	224 x 224 pixels
Training-Validation Split	80:10:10(training: Validation: Testing)
Dropout Rate	0.2
Learning Rate	0.001
Epochs	20
Batch Size	32
Optimizer	Adam
Loss Function	Categorical Cross-Entropy
Activation Function	Softmax
Model Architecture	EfficientNet-B0
Pre-trained Weights	ImageNet
Data Augmentation	Rotation, Zoom, Jitter, Flip

The learning rate is set to 0.001, which is a standard choice. To train this model for 20 epochs with a batch size of 32. Here, a multi-class classification problem is used with the Adam optimizer, which is used to update the weights. Here, the data augmentation technique is used, such as zoom jittering and flipping, to increase the data variety, which helps in analysing the model to generalize better for new and unseen data.

Sample Images of Mulberry Root Knot Disease Classification Based on Leaf Symptoms

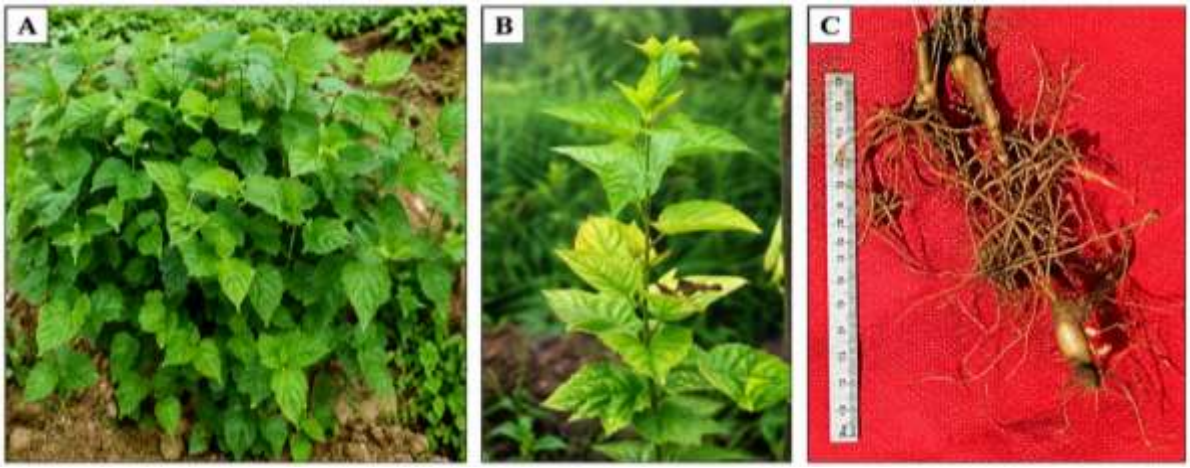

A. Stunted growth; B. Yellowing and marginal necrosis; C. Root-knots

Figure 5. Mulberry root disease classification based on leaf symptoms

The figure 5 above demonstrates three varying states of mulberry plants that exhibit varying disease symptoms. Figure 5A depicts a healthy mulberry plant characterized by rich green coloration of the leaves with no indication of any disease. Figure 5B demonstrates a diseased mulberry plant suffering from symptoms such as yellowed and marginally necrotic leaves, indicating an infection due to fungi or bacteria that may be caused by root-knot nematodes or wilts. Figure 5C shows the roots of a diseased mulberry plant that exhibits damage due to root-knot nematode disease. This visual illustration plays an important role in understanding the impact of root-borne diseases on mulberry plants that is fundamental in managing the disease [25].

Sample Images-Input Images

Figure 6. Sample input images

Sample Images-Output Images

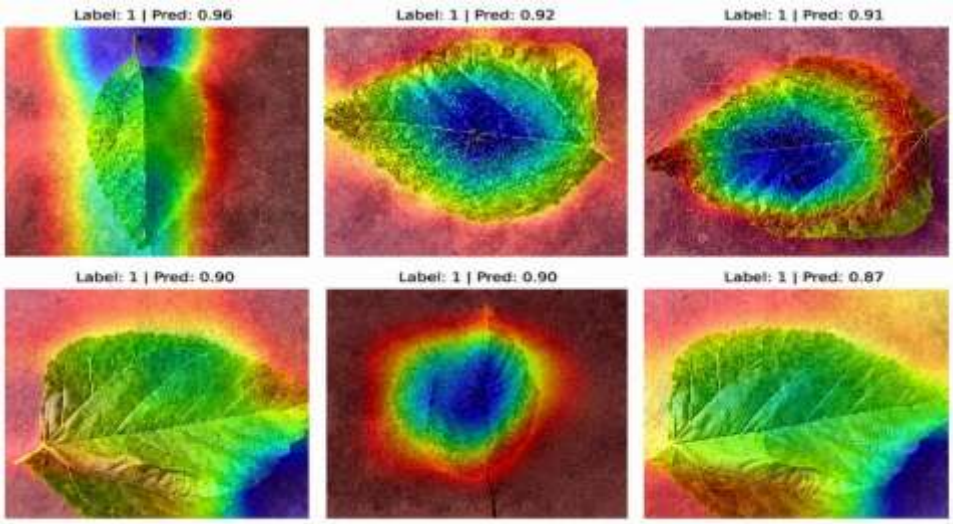

Figure 7. Sample output images

The following figure 6 and figure 7 are used to provide a comparison between the input and output results in mulberry root knot disease classification. First, the Sample Input Images consist of various leaf states, including healthy and disease-infected leaves with varying symptoms. The Sample Input Images are then used by the model to classify the various diseases through analysing their leaf symptoms. On the other hand, the Sample Output Images are used to represent the various Grad-CAM visualizations. In this case, the Grad-CAM visualizations have been applied to each image of the leaves, with heat maps being overlaid in the areas where the model paid particular attention during the classification process. The Label column contains the actual leaf class, while the Pred column represents the confidence score prediction of the model.

Metric Evaluation of Various Models

Various evaluation metrics were used to measure the performance of the developed model with respect to the model's performance, including area under the curve (AUC), recall (R), accuracy (ACC), and precision (P). The percentage of correctly detected images to the total number of photographs is called "accuracy". It showed the effectiveness of the classification system for the identification of leaf Root Knot diseases. When a disease-infected leaf is correctly classified as infected, it is a true positive (TP).

A false positive (FP) is when a healthy leaf is mistaken for having the disease, and a false negative (FN) is when the patient has no disease. Between equations 5, 6 and 7, 8 are several measures of performance defined.

$$Accuracy(A) = TP + TN/TP + TN + FP + FN \quad (5)$$

$$Precision(P) = {}^{TP}/_{TP + FP} \quad (6)$$

$$Recall(R) = {}^{TP}/_{(TP + FN)} \quad (7)$$

$$F1Score(F1) = 2 * Recall * \frac{Precision}{Recall} + Precision \quad (8)$$

Performance Comparison for the Proposed Model with the Various Models

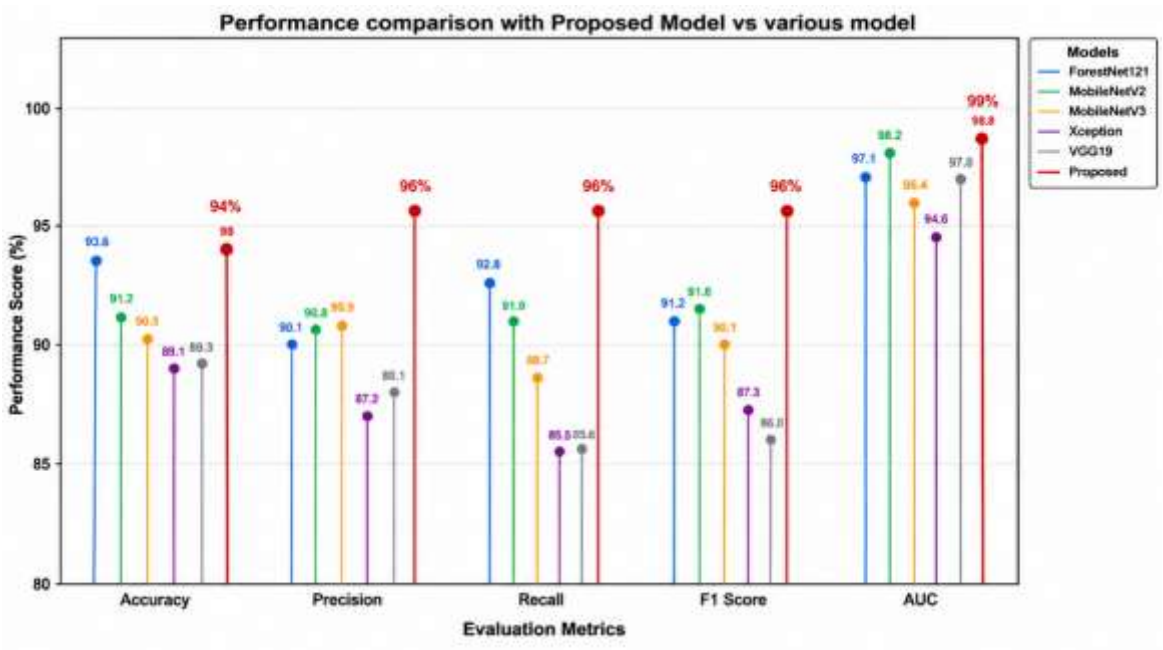

Figure 8. Performance comparison with the proposed model Vs various model

Figure 8 shows the performance analysis of the proposed model as compared to other models, including DenseNet121, MobileNet, MobileNetV3, Xception, and VGG19 in terms of different criteria, including A, P, R, F1, and AUC (Area Under Curve). It can be seen from figure 8 that the proposed model outperformed all the models under comparison with significant improvement in terms of all the criteria used. Particularly, the proposed model scored 94% in terms of accuracy, which is equal to previous models. So, maintain the same accuracy in this research. In addition, the proposed model obtained the maximum performance in terms of P, R, F1, and AUC as well, scoring 95% in each of the mentioned criteria. Hence, it can be concluded that the proposed model outperformed other models in terms of classification accuracy and positive cases identification. It was also noted that compared to the other models like VGG19 and Xception, the proposed model excels in performance [31].

Performance Evaluation of Proposed Model

The performance evaluation plot figure 9, shows the outcome of several performance evaluation criteria applied to a specific model. All these criteria including A, P, R, F1, and AUC, have been scored. It can be seen from the graph that performance is outstanding for each of the measures. The maximum score is that of AUC, which is 0.99; hence, indicating an excellent ability of the model to discriminate. On the other hand, P, R, and F1 are all equal at 0.95; therefore, suggesting a balanced capacity by the model to

detect both positive and negative classes. Accuracy, too, is relatively high at 0.94, implying that the model makes correct predictions for most cases.

Figure 9. Performance evaluation of the proposed methodology

ROC Curve Evaluation

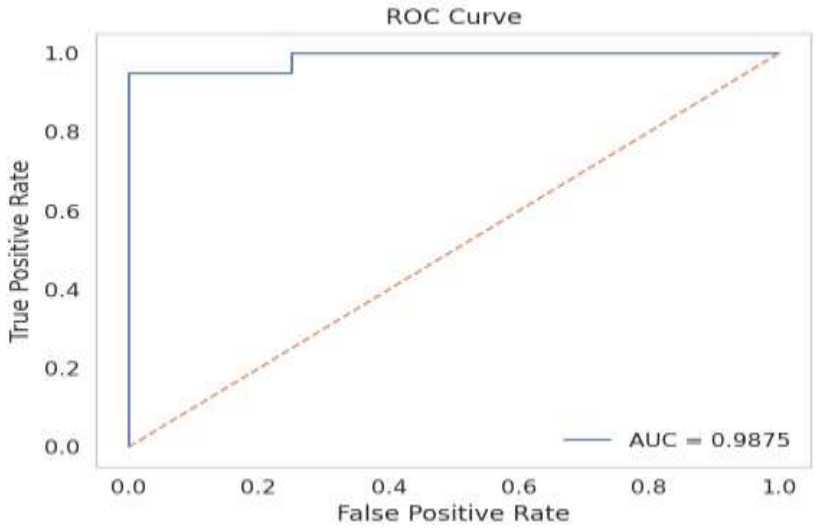

Figure 10. ROC curve evaluation

It is possible to observe the trade-offs between the True Positive Rate (TPR) and the False Positive Rate (FPR) in the ROC graph that is presented below in figure 10. This ROC curve graph offers a graphical depiction of the model's capacity to differentiate between different types of data. Given that the Area Under the Curve (AUC) is 0.9875, it can be concluded that the model has given satisfactory results. Followed by AUC, which indicates the model has a positive value should be positive.

Training Accuracy

The accuracy plot figure 11 gives the training accuracy of the model during the 20 epochs. The above plot demonstrates an increasing accuracy trend as the number of epochs advances, with the model steadily improving. The accuracy starts at about 0.55 at the start of the training and ends up being about 0.80 at the 20th epoch. This plot shows that the model is improving, and this is demonstrated by its

accuracy trend. The significant jumps at some specific epochs could show fast learning at that point, while the gradual increments could indicate progressive learning.

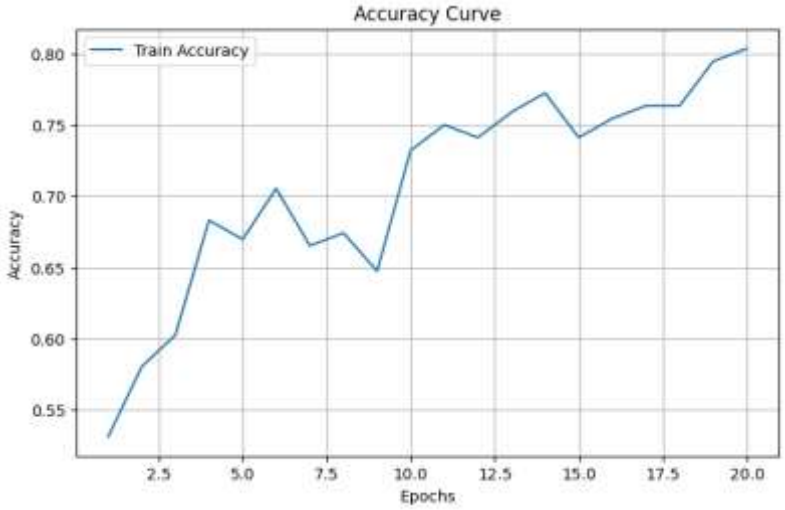

Figure 11. Training accuracy

Training Loss

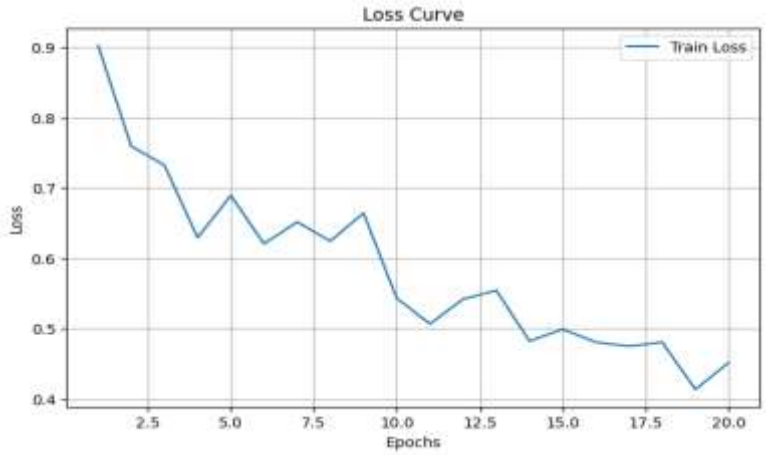

Figure 12. Training loss

The loss graph shows the training loss for the model for 20 epochs. The loss falls gradually from about 0.9 at the beginning of the training process to 0.4 in the 20th epoch in figure 12. It means that the model becomes better at prediction, and the loss is getting lower, which is a sign of reducing the error. In the first few epochs, there is a steep decrease in the graph, meaning that the model is experiencing good learning. After that, there is a steady decrease in the graph; however, some fluctuations can be noticed during specific epochs. Nevertheless, the general trend of the graph remains decreasing, indicating convergence of the model.

Ablation Study Analysis

The performance of four model variants—Full Model, Eff + Res, Res Only, and Eff Only—is compared in the ablation research figure 13, using four measures: Accuracy, Precision, Recall, and F1 Score. The models reflect their configurations. Within each of the four criteria, the Full Model beats competing models, with a particular emphasis on its superior performance in the areas of Recall and F1 Score. According to this, it appears that the model achieves the best possible equilibrium when it takes into account both the positive and negative classes in its forecast. The Eff + Res Model performs slightly

worse than the Full Model and is comparable with other models in all measures except Recall, where it outperforms the remaining models.

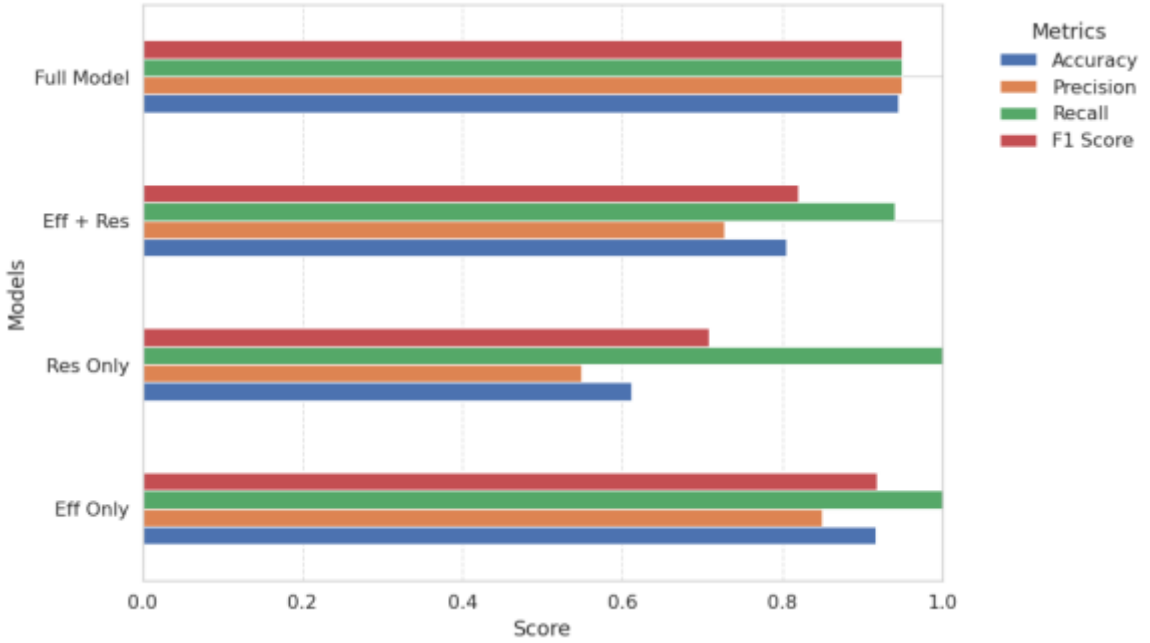

Figure 13. Ablation study comparison

This can be attributed to the fact that the combination of both Eff and Res contributes to its good performance. Conversely, when contrasted with other model variants, the Res Only model performs poorly across the board, especially in terms of Accuracy, Precision, and F1 Score. In light of this, it appears that concentrating solely on Resolution is not an adequate method for reaching the highest possible level of model performance. Eff Only Model performs better than Res Only Model, but it fails miserably when it comes to Precision and F1 Score, suggesting that efficiency isn't enough to get optimal results.

CONCLUSION

The EfficientMulberryNet-B0-GC is a novel artificial intelligence (AI) model for the automated diagnosis of mulberry root knot illness using symptoms observed on the leaves. It is proposed in this work. In order to make the model more accurate and easier to understand, this updated version makes use of EfficientNet-B0 and Grad-CAM visualization. The EfficientMulberryNet-B0-GC achieved higher performance than all other competing models: 94% accuracy, 95% precision, 95% recall, 95% F1 score, and 99% area under the curve. The results obtained from the present model show its effectiveness in detecting root knot disease of mulberry in the agricultural environment. Using Grad-CAM visualization for the model can improve the interpretability of the model as well as understanding the model's decision-making process. The further study can be based on the existing data set of mulberry leaves, which is small, and make it larger and more effective to build models. Additionally, it will be fascinating to investigate how other pre-trained AI models can be incorporated to increase the accuracy of disease classification. Besides, the AI model developed in this study can be applied in the smart farming system to automatically detect leaf root knot disease in mulberry orchards.

Acknowledgement:

This Research Work is Supported by the Department of Science Technology (DST), Govt. of India.

REFERENCES

[1] Hasan MA, Haque F, Sarker H, Abdullah R, Roy T, Taaha N, Arafat Y, Patwary AK, Ahsan M, Haider J. Mulberry leaf disease detection by CNN-ViT with XAI integration. PLoS One. 2025 Jun 4;20(6):e0325188. https://doi.org/10.1371/journal.pone.0325188

[2] Devi K, Benila S, Lekshmi K, Omana J. HVAF-XAI-net: A multimodal explainable AI framework for accurate mulberry leaf disease detection. Smart Agricultural Technology. 2025 Aug 29:101377. https://doi.org/10.1016/j.atech.2025.101377

[3] Meerasha B, Sagayam KM, Bruntha PM, David J, Koduri V. Advanced Soft Computing Paradigm for Crop Mapping Using Remote Sensing and Artificial Intelligence: a review. Archives for Technical Sciences. 2025 Dec 1(34):1297-1306. https://doi.org/10.70102/afts.2025.1834.1297

[4] Kaler B, Kaur A. A systematic survey on explainable artificial intelligence (XAI) for plant health monitoring: challenges and opportunities. Applied Intelligence. 2025 Aug;55(12):889. https://doi.org/10.1007/s10489-025-06790-x

[5] Gopalan K, Srinivasan S, Singh M, Mathivanan SK, Moorthy U. Corn leaf disease diagnosis: enhancing accuracy with resnet152 and grad-cam for explainable AI. BMC Plant Biology. 2025 Apr 7;25(1):440. https://doi.org/10.1186/s12870-025-06386-0

[6] Nithyalakshmi V, Sivakumar R, Sivaramakrishnan A. Automatic detection and classification of diabetes using artificial intelligence. International Academic Journal of Innovative Research. 2021 Dec 20;8(1):01-5. https://doi.org/10.9756/IAJIR/V8I1/IAJIR0801

[7] Yuan C, Li S, Wang K, Liu Q, Li W, Zhao W, Guo G, Wei L. Mamba-yolo-ml: A state-space model-based approach for mulberry leaf disease detection. Plants. 2025 Jul 7;14(13):2084. https://doi.org/10.3390/plants14132084

[8] Abirami G, Nandhini SA. Fusion-Based CNN Ensemble with Grad-CAM for Trustworthy and Transparent Plant Disease Detection. AI Trust, Risk, and Security Management: Framework, Principles, and Practices. 2026 Jan 20:73-98.

[9] Fu Y, Sun DW. Advancing Fruit Quality Monitoring with Artificial Intelligence-Augmented Non-Destructive Technologies. Food Engineering Reviews. 2026 Jun;18(2):9. https://doi.org/10.1007/s12393-026-09437-w

[10] Sadasivam VR, Shaheen H, Kishore KH. Hybrid knowledge-based and data-driven explainable AI architectures for intelligent fault diagnosis in cyber-physical systems. International Academic Journal of Science and Engineering. 2025;12(3):394-404. https://doi.org/10.71086/IAJSE/V12I3/IAJSE1275

[11] Wu Q, Chen Y, Meng J. DCGAN-based data augmentation for tomato leaf disease identification. IEEE access. 2020 May 25;8:98716-28. https://doi.org/10.1109/ACCESS.2020.2997001

[12] Chen H, Wang Y, Jiang P, Zhang R, Peng J. LBFNet: A tomato leaf disease identification model based on three-channel attention mechanism and quantitative pruning. Applied Sciences. 2023 Apr 30;13(9):5589. https://doi.org/10.3390/app13095589

[13] Mishra, N., Haval, A. M., Mishra, A., & Dash, S. S. (2024). Automobile Maintenance Prediction Using Integrated Deep Learning and Geographical Information System. Indian Journal of Information Sources and Services, 14(2), 109–114. https://doi.org/10.51983/ijiss-2024.14.2.16

[14] Khattak A, Asghar MU, Batool U, Asghar MZ, Ullah H, Al-Rakhami M, Gumaei A. Automatic detection of citrus fruit and leaves diseases using deep neural network model. IEEE access. 2021 Jul 13;9:112942-54. https://doi.org/10.1109/ACCESS.2021.3096895

[15] Dhanya R, Mythili S. Enhanced tomato leaf disease detection using Inception V3 with dual attention mechanisms. Journal of Wireless Mobile Networks, Ubiquitous Computing, and Dependable Applications. 2025;16(4):402-426. https://doi.org/10.58346/JOWUA.2025.I4.023

[16] Khan GM, Khan MR, Mondal S, Sasmal P. Machine Learning-Based Identification of Root-Knot Nematodes (Meloidogyne spp.) at the Species Level Using Microscopic Images. Journal of Phytopathology. 2025 Nov;173(6):e70212. https://doi.org/10.1111/jph.70212

[17] Das S, Ghosh K, Mondal S, Dutta S, Khan MR, Garain U, Mukherjee A. A deep learning framework for species-level identification of root-knot nematodes using perineal pattern images. Scientific Reports. 2026 Jan 8;16(1):3180. https://doi.org/10.1038/s41598-025-33143-y

[18] Zhao Y, Zhao H, Xiong H, Zhang F, Lu C, Li J. Root-YOLOv7: Multi-scale adaptive object detection and grading of root-knot nematode disease. International Journal of Agricultural and Biological Engineering. 2025 Apr 30;18(2):259-68. https://doi.org/10.25165/j.ijabe.20251802.9414

[19] Rangarajan V, Shahoveisi F, Waldo BD, Jafari S. Identification of plant-parasitic nematode genera in turfgrass using deep learning algorithms. Scientific Reports. 2025 Dec 7;16(1):24. https://doi.org/10.1038/s41598-025-29467-4

[20] Singh N, Singh AK, Dhruw LK, Kaur S, Hazarika S, Mishra KK, Mishra VK, Kant L. Development of a Deep Learning-Assisted Mobile Application for the Identification of Nematodes Through Microscopic Images. Modern Agriculture. 2024 Dec;2(2):e70000. https://doi.org/10.1002/moda.70000

[21] Saikai KK, Bresilla T, Kool J, de Ruijter NC, Van Schaik C, Teklu MG. Counting nematodes made easy: leveraging AI-powered automation for enhanced efficiency and precision. Frontiers in plant science. 2024 Jun 26;15:1349209. https://doi.org/10.3389/fpls.2024.1349209

[22] Fraher SP, Watson M, Nguyen H, Moore S, Lewis RS, Kudenov M, Yencho GC, Gorny AM. A comparison of three automated root-knot nematode egg counting approaches using machine learning, image analysis, and a hybrid model. Plant Disease. 2024 Sep 1;108(9):2625-9. https://doi.org/10.1094/PDIS-01-24-0217-SR

[23] Pun TB, Neupane A, Koech R, Walsh K. Detection and counting of root-knot nematodes using YOLO models with mosaic augmentation. Biosensors and Bioelectronics: X. 2023 Dec 1;15:100407. https://doi.org/10.1016/j.biosx.2023.100407

[24] Pun TB, Neupane A, Koech R. A deep learning-based decision support tool for plant-parasitic nematode management. Journal of Imaging. 2023 Nov 6;9(11):240. https://doi.org/10.3390/jimaging9110240

[25] Pun TB, Thapa Magar R, Koech R, Owen KJ, Adorada DL. Emerging trends and technologies used for the identification, detection, and characterisation of plant-parasitic nematode infestation in crops. Plants. 2024 Oct 30;13(21):3041. https://doi.org/10.3390/plants13213041

[26] Waghmare CD. Hyperspectral Remote Sensing Detection of Root-Knot Nematode Infestation in Mungbean under Various Management Strategies: Hyperspectral Remote Sensing of Root-Knot Nematode in Mungbeans. Journal of Scientific & Industrial Research (JSIR). 2024 Mar 7;83(3):309-14. https://doi.org/10.56042/jsir.v83i3.3662

[27] Lapajne J, Knapič M, Žibrat U. Comparison of selected dimensionality reduction methods for detection of root-knot nematode infestations in potato tubers using hyperspectral imaging. Sensors. 2022 Jan 4;22(1):367. https://doi.org/10.3390/s22010367

[28] Pun TB, Neupane A, Koech R. Quantification of root-knot nematode infestation in tomato using digital image analysis. Agronomy. 2021 Nov 23;11(12):2372. https://doi.org/10.3390/agronomy11122372

[29] Gómez-Flores W, Garza-Saldaña JJ, Varela-Fuentes SE. A huanglongbing detection method for orange trees based on deep neural networks and transfer learning. IEEE Access. 2022 Nov 4;10:116686-96. https://doi.org/10.1109/ACCESS.2022.3219481

[30] Masood M, Nawaz M, Nazir T, Javed A, Alkanhel R, Elmannai H, Dhahbi S, Bourouis S. MaizeNet: A deep learning approach for effective recognition of maize plant leaf diseases. IEEE Access. 2023 May 26;11:52862-76. https://doi.org/10.1109/ACCESS.2023.3280260

[31] Salam A, Naznine M, Jahan N, Nahid E, Nahiduzzaman M, Chowdhury ME. Mulberry leaf disease detection using CNN-based smart android application. IEEE Access. 2024 May 30;12:83575-88. https://doi.org/10.1109/ACCESS.2024.3407153